Journal of Physics: Conference Series

Analysis of magnetic field characteristics and no-load losses of three-dimensional wound core transformer

To cite this article: Min Li *et al* 2023 *J. Phys.: Conf. Ser.* **2503** 012073

Analysis of magnetic field characteristics and no-load losses of three-dimensional wound core transformer

Min Li[1], Wei Yao[1], Xin Gao[1], Cong Liu[2a*]

[1]China State Grid Taiyuan Power Supply Company, Taiyuan 030000, China

[2]School of Electrical Engineering, Shandong University, Jinan 250100, China

[a*]congliu2019@mail.sdu.edu.cn

Abstract: Three-dimensionally wound core transformers (TWCTs) are widely used because of their low iron loss. This paper investigates the triangularly arranged TWCT core structure and a conventional planar laminated core transformer's flat "E" core structure (PLCT). First, the magnetic field structures of the two transformers are analyzed using the equivalent magnetic circuit method to study the symmetry of the three-phase reluctance. Then, using the finite element method, a three-dimensional simulation model was built to analyze the no-load performance of TWCT and PLCT with the same dimensional parameters and the same core material. The no-load flux of each coil, the induced voltage on the secondary side, and the no-load iron loss of the core are analyzed. The analysis results show that TWCT has a 7.48% lower no-load loss than PLCT, which verifies the superiority of TWCT in terms of no-load loss.

1. Introduction

As an important part of the power system, transformers play an important role in power transmission, transformation, and distribution [1]. The total power loss of transformers accounts for about 10% of the power generation capacity of the power plant, so the size of its loss directly affects the economy of grid operation. As one of the sources of loss, no-load loss accounts for a certain proportion of the total loss of the transformer. The no-load losses of transformers mainly include hysteresis, eddy current, and additional losses, collectively referred to as iron loss. The iron loss of the transformer is not related to the load size but is mainly determined by the structure of the transformer, core temperature, core material, and processing technology [2].

There are many different types of three-phase transformer structures, and the commonly used structures are PLCT and TWCT [3][4]. Compared with the traditional PLCT, the TWCT core has the advantages of low loss and noise due to the uniform distribution of the magnetic circuits, complete symmetry of the three-phase magnetic circuit, and complete balance of no-load current [5][6]. At the same time, PLCT laminated cores produce local oversaturation of flux at the joints due to magnetic field distortion, which can lead to large iron loss [7]. Due to the processing of rolled cores, TWCT is often rolled from low-loss iron-based nanocrystalline materials or amorphous alloy strips. The strips are tightly wound with each other, and the cores are closed-ended structures without laps and joints, resulting in a significant reduction in iron loss [8][9].

This paper analyzes PLCT and TWCT with the same geometry and core material to investigate the effect of PLCT planar "E" core and TWCT triangular core structure on transformer losses. To verify the advantages of TWCT, the comparison between TWCT and PLCT is carried out from the aspects of transformer structural characteristics, magnetic circuit analysis, electromagnetic characteristics, and loss analysis.

2. Structure of transformers

The core of the PLCT is "E" shaped, and the three-phase windings are located on three core columns, as shown in Figure 1(a). Since the core is a flat structure, the three phases of the magnetic circuit length are not equal. The middle B phase is shorter, and the two sides of the A and C phases are longer, resulting in a slight difference in the three-phase reluctance. When the external applied three-phase symmetric voltage, the three-phase no-load currents will not be equal, with the B-phase current slightly smaller and the A and C phases larger.

The core structure of TWCT consists of three single core frames with identical geometric dimensions combined at 60 degrees to each other, and a three-phase core column is formed by two adjacent frame edges, as shown in Figure 1(b). Due to the identical structure of the three single frames, the core structure is centrally symmetric, and the three-phase reluctance is the same. The three-phase no-load current is also symmetric when the three-phase symmetric voltage is applied externally. The triangular three-dimensional core structure is symmetrical to each other, and there is no joint in the middle of every single frame of the core, forming a closed structure.

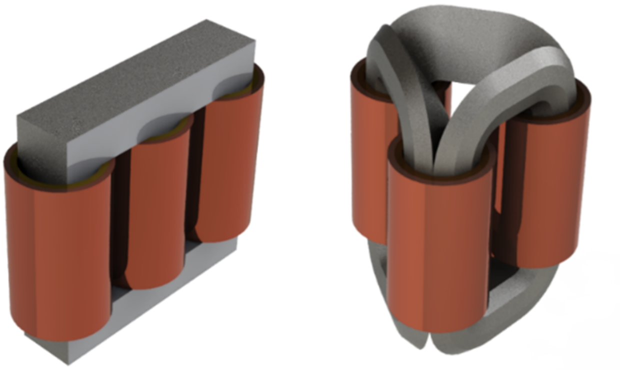

(a) PLCT (b) TWCT

Figure 1 The topology of the transformer

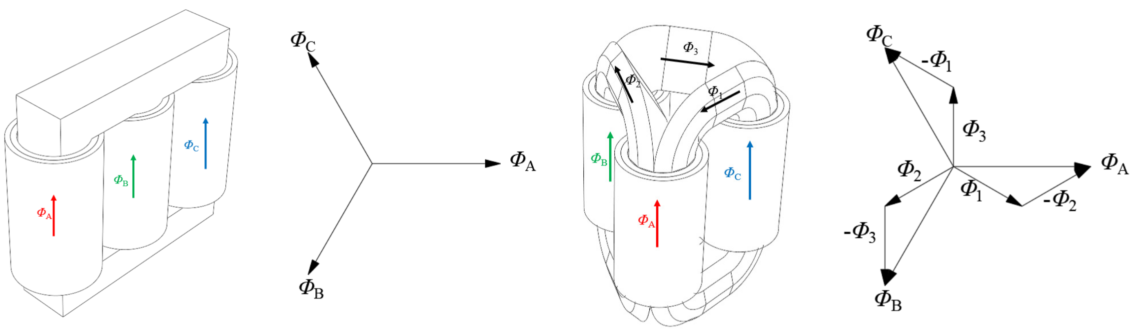

(a) PLCT (b) TWCT

Figure 2 Magnetic circuit and flux vector diagram

Figure 2 shows the position and vector of three-phase flux linkage in the transformer. In the magnetic transformer circuit, the average fluxes in the core columns of phase A, phase B, and phase C are Φ_A, Φ_B, and Φ_C. For PLCT, there are only two flux loops in the core. And for TWCT, the fluxes flowing in the three core single frames are Φ_1, Φ_2, and Φ_3, respectively. The magnetic circuit diagram of the transformer is shown in Figure 3.

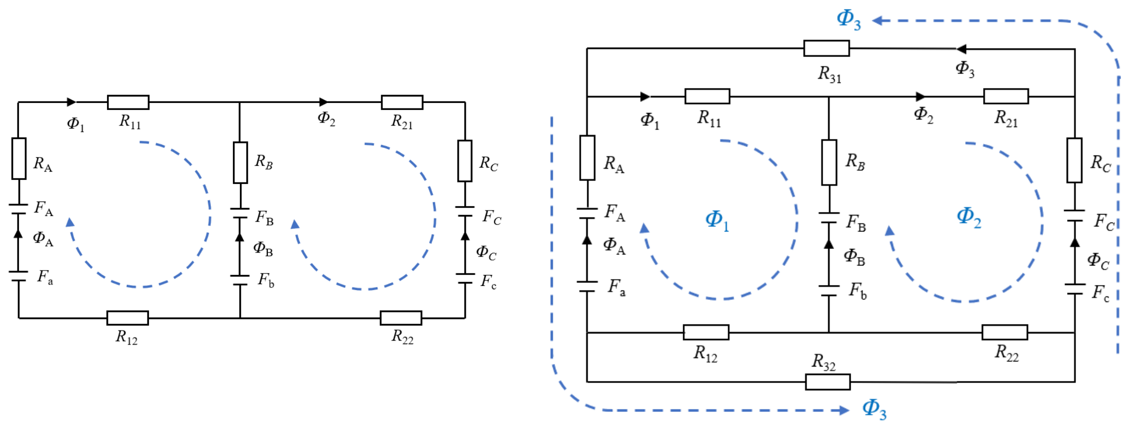

(a) PLCT (b) TWCT

Figure 3 Magnetic circuit diagram

R_A, R_B, and R_C are the reluctance in the core column. The reluctance at the top of the core is represented by R_{11} to R_{32}. F_A, F_B, and F_C are the magnetic potentials provided by the primary coil. F_a, F_b, and F_c are the magnetic potentials of the secondary coil. Due to the symmetry of the transformer core structure, the equation can be obtained: R_A=R_B=R_C, R_{11}=R_{12}=R_{21}=R_{22}=R_{31}=R_{32}. In PLCT, the reluctance of the three phases of A, B, and C are listed in (1).

$$\begin{aligned} R_{\mathrm{eqA}} &= R_{\mathrm{A}} + R_{11} + R_{12} + R_{\mathrm{B}} // (R_{21} + R_{22} + R_{\mathrm{C}}) \\ R_{\mathrm{eqB}} &= R_{\mathrm{B}} + (R_{11} + R_{12} + R_{\mathrm{A}}) // (R_{21} + R_{22} + R_{\mathrm{C}}) \\ R_{\mathrm{eqC}} &= R_{\mathrm{C}} + R_{21} + R_{22} + R_{\mathrm{B}} // (R_{11} + R_{12} + R_{\mathrm{A}}) \end{aligned} \tag{1}$$

It can be found that in PLCT, R_{eqA} = $R_{eqC} \neq R_{eqB}$. In TWCT, the reluctance of the three phases of A, B, and C are listed in (2).

$$\begin{aligned} R_{\mathrm{eqA}}' &= R_{\mathrm{A}} + \frac{2}{3}R_{11} + (R_{\mathrm{B}} + \frac{2}{3}R_{11}) // (R_{\mathrm{C}} + \frac{2}{3}R_{11}) \\ R_{\mathrm{eqC}}' &= R_{\mathrm{C}} + \frac{2}{3}R_{11} + (R_{\mathrm{A}} + \frac{2}{3}R_{11}) // (R_{\mathrm{B}} + \frac{2}{3}R_{11}) \\ R_{\mathrm{eqB}}' &= R_{\mathrm{B}} + \frac{2}{3}R_{11} + (R_{\mathrm{A}} + \frac{2}{3}R_{11}) // (R_{\mathrm{C}} + \frac{2}{3}R_{11}) \end{aligned} \tag{2}$$

In TWCT, R_{eqA}’ =R_{eqB}’=R_{eqC}’, and the three-phase reluctance is the same. The difference in core structure is the fundamental reason for the difference in no-load losses between the two transformer structures.

3. Finite element method of magnetic field analysis

To further analyze the no-load performance of the two transformers, the three-dimensional finite element analysis model is established for magnetic field analysis. The transformer shell, insulation material, and support structure are ignored in the model to reduce the computational analysis time. To avoid the influence of the transformer core material on the structural performance of the transformer, the material used for the TWCT core is the same as that used for the PLCT core. The height, width, cross-sectional area, and other parameters of the transformer cores of both structures are the same, and the relevant parameters are listed in Table 1.

Table 1 Specifications of the power transformer model

Classification	Unit	Value
Core single-frame height	mm	400
Core single frame width	mm	187
Core column cross-sectional area	mm^2	8356
Frequency	Hz	50
Primary Turns	Turns	200
Secondary Turns	Turns	20
Core material	/	50JN270

Based on the parameters in Table 1, a three-dimensional simulation model is established in the finite element simulation software. The primary winding of the transformer is connected to a three-phase voltage with a frequency of 50 Hz and an RMS value of 100 V, and the electromagnetic performance of the transformer is analyzed. To study the no-load performance of the transformer, the secondary side winding of the transformer is disconnected, and the magnetic density distribution diagram of the transformer is shown in Figure 4.

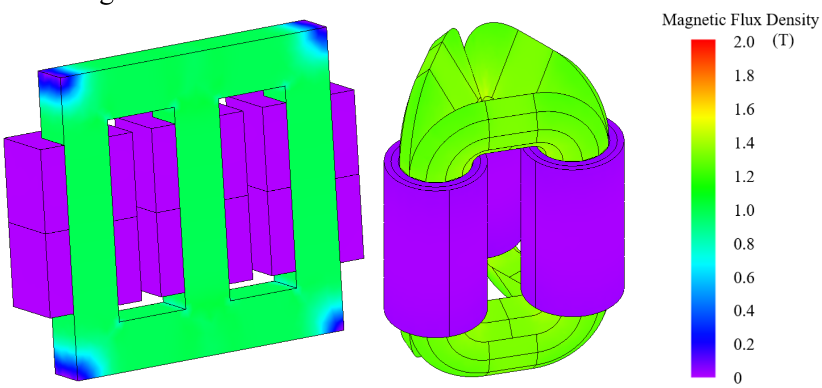

(a) PLCT (b) TWCT

Figure 4 No-load magnetic density distribution of transformer

The maximum magnetic flux density in PLCT is 1.45 T, and the maximum magnetic flux density in TWCT is 1.49 T. Except for the edges of the PLCT core, the magnetic flux density in the transformer core is above 1.0 T, and the transformer core is almost completely utilized. The coil flux linkage through each winding in PLCT and TWCT is shown in Figure 5.

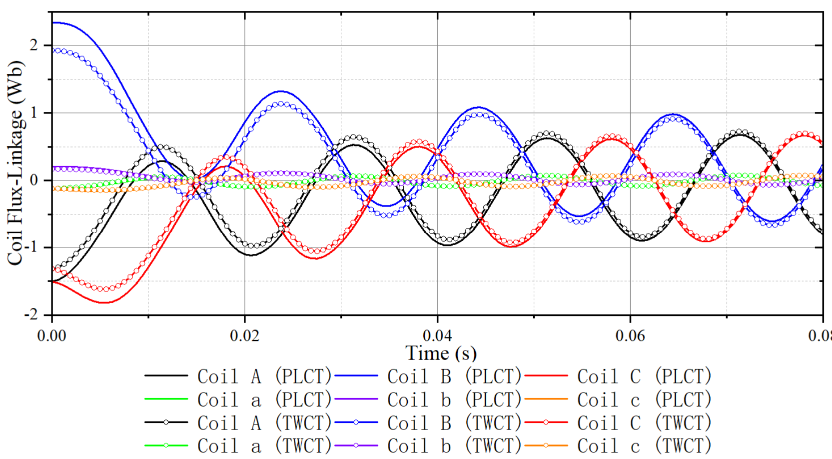

Figure 5 The coil flux linkage of windings

The primary coils of the transformer are coil A, coil B, and coil C, and the secondary coils are coil a, coil b and coil c. From the flux of each coil, there is a gradual decay of the flux of the primary winding after the transformer is connected to a three-phase power supply, which eventually tends to a steady state gradually. The flux of the secondary winding is always more stable. On the other hand, the flux of each primary coil in the PLCT is larger than that in the TWCT during transients. After stabilization, they are almost the same.

Periodic variations in the transformer magnetic field produce induced voltages in the transformer's secondary winding. The transformer no-load voltage comparison is shown in Figure 6.

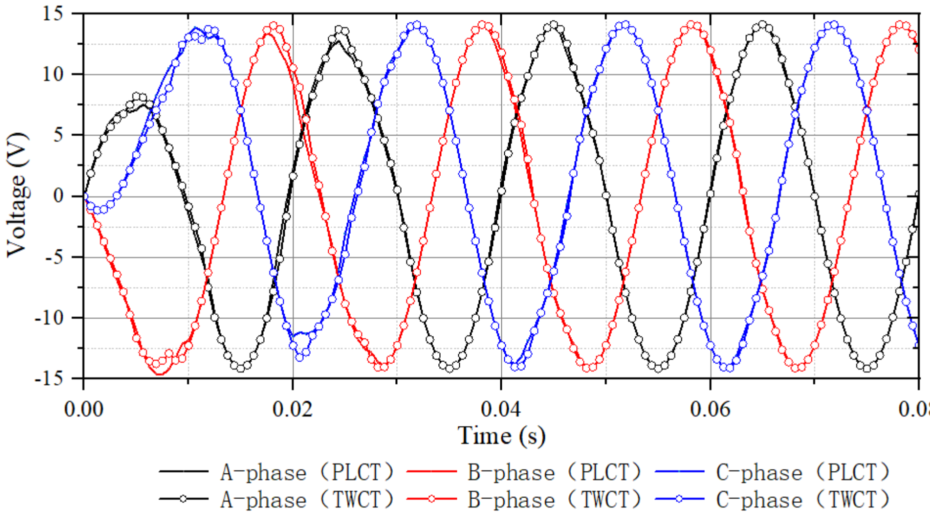

Figure 6 No-load voltage of the secondary winding of the transformer

Due to the transformer's primary and secondary turns ratio being 10:1, the stable voltage amplitude induced on the secondary side of the transformer at no load is 14.14 V, and the rms value is 10 V. The comparison of transformer iron loss density clouds, as shown in Figure 7. And the no-load loss data obtained in the simulation are shown in Table 2.

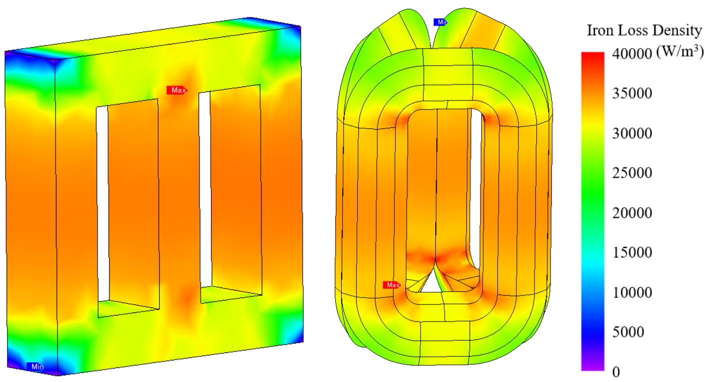

Figure 7 No-load iron loss density cloud of transformer

Table 2 No-load losses in transformers model

Classification	Unit	Value
The maximum loss density of PLCT	W/m^3	400
The total no-load loss of PLCT	W	187
The maximum loss density of TWCT	W/m^3	8356
The total no-load loss of TWCT	W	50

The maximum loss density point in PLCT is 41664 W/m^3 and the total no-load loss is 443.6 W, while the maximum loss density point in TWCT is 39988 W/m^3 and the total no-load loss is 415.4 W, which is 7.48% lower than PLCT.

4. Conclusion

This paper analyzes the structure and magnetic circuit characteristics of the triangular core of TWCT and the flat “E” core of a PLCT. And the three-dimensional finite element simulation is used to verify and analyze the no-load performance of TWCT and PLCT with the same dimensional parameters and core material. The analysis focuses on the no-load secondary induced voltage and no-load iron loss. The simulation results show that the no-load losses are 443.6 W for PLCT and 415.4 W for TWCT. 7.48% less than PLCT under the same conditions.

Acknowledgments

This work was supported by the Science and Technology Project of State Grid Shanxi Electric Power Company 5205A0220003.

References

[1] Y. WU, L. LIU, C. SHI, K. MA, Y. LI and H. MU. (2019) Research on Measurement Technology of Transformer No-load Loss Based on Internet of Things. In: 2019 IEEE 8th International Conference on Advanced Power System Automation and Protection (APAP), Xi’an, China, pp. 150-153.
[2] R. Arseneau, E. So and E. Hanique. (2005) Measurements and correction of no-load losses of power transformers. In: IEEE Transactions on Instrumentation and Measurement, vol. 54, no. 2, pp. 503-506.
[3] G. Upadhyay, A. Singh, S. K. Seth and R. K. Jarial. (2016) FEM-based no-load loss calculation of triangular wound core transformer. In: 2016 IEEE 1st International Conference on Power Electronics, Intelligent Control and Energy Systems (ICPEICES), Delhi, India, pp. 1-4.
[4] G. Liu, C. Liu, X. Xiong. et al. (2020) Simulation of the Magnetic Field Distribution and Voltage Error Characteristics of the Three-Phase Three Component Combined Transformer with New Three-Cylinder Core Structure. In: IEEE Transactions on Magnetics.
[5] X. Huang. (2009) H-class Dry-type Transformer with Three-dimensional D-form Rolled Core. In: Guangdong Electric Power.
[6] B. Yang, X. Fan. et al. (2022) Modeling and No-Load Characteristics Analysis of 3D Wound Core Transformer Considering Core Nonlinearity. In: Transactions of China Electrotechnical Society.
[7] H. Zhang. (2017) Research and application of three-dimensional rolled-iron core combined transformer for the wind farm. In: Shandong University of Science and Technology.
[8] S. Duan. (2021) Electromagnetic performance analysis and loss calculation of three-phase winding core transformer. In: Shenyang University of Technology.
[9] A. Moradnouri, P. Elhaminia and M. Vakilian. (2015) Amorphous metal triangular cores to improve distribution transformers design. In: International Transformer Conference and Exhibition, Tehran, pp. 1-5.